

mass difference between the hyperon and the nucleon is disregarded in deriving the potential but not in the kinematics.

<sup>6</sup> See Fig. 5 of the second SM paper, reference 1.

<sup>7</sup> See R. H. Dalitz, Reports on Progress in Physics (The Physical Society, London, 1957), Vol. 20, p. 163.

<sup>8</sup> Taking account of the admixture of  $^3D_1$  with  $^3S_1$  should not appreciably modify the cutoff, since the tensor force is small compared to the central part of the SM potential.

<sup>9</sup> See M. Gell-Mann and A. Rosenfeld, Annual Review of Nuclear Science (Annual Reviews, Inc., Stanford, 1957), Vol 7, p. 407.

<sup>10</sup> Some preliminary evidence comes from a study of the reaction  $K^- + p$  [see A. Fujii and R. Marshak, Nuovo cimento (to be published)]; other arguments are given in M. Gell-Mann and A. Rosenfeld, reference 9, and A. Pais, Phys. Rev. **110**, 574 (1958).

### OPTICAL MODEL POTENTIAL AT THE NUCLEAR SURFACE FOR THE ELASTIC SCATTERING OF ALPHA PARTICLES \* George Igo

Los Alamos Scientific Laboratory,  
Los Alamos, New Mexico, and  
Stanford University, Stanford, California  
(Received June 9, 1958)

The elastic scattering of 18-Mev alpha particles from argon,<sup>1</sup> 40-Mev alpha particles from copper,<sup>2</sup> and 48-Mev alpha particles from lead<sup>3</sup> has been analyzed in terms of the optical model. A radial nuclear potential<sup>4</sup>  $(V + iW)/\{1 + \exp[(r - r_0)/d]\}$  and a radial charge distribution  $\rho(r)$  of the form<sup>5</sup>

$$\rho(r) \sim 1 - \frac{1}{2} \exp[n(r/r_0 - 1)], \quad r \leq r_0$$

$$\sim \frac{1}{2} \exp[n(1 - r/r_0)], \quad r \leq r_0$$

have been employed. This method of analysis is by now very familiar and will not be described here.<sup>6</sup>

In previous work<sup>6</sup> we have mainly tested the family of nuclear potentials generated by changing  $V$  and  $W$  while keeping  $r_0$  and  $d$  equal to  $1.37A^{1/3} + 1.30$  and  $0.5$  fermis, respectively (1 fermi =  $10^{-13}$  cm). We had found best average values of  $V$  and  $W$  to be about  $-45$  Mev and  $-10$  Mev for all elements considered at bombarding energies of 22<sup>7</sup> and 40 Mev.<sup>2, 8</sup> Cheston and Glassgold<sup>9</sup> have pointed out that it is probably possible to fit the data with potentials resulting from other values of  $r_0$  and  $d$ .

The family of nuclear potentials which can be generated by changing all four parameters was

employed in the present analysis. Since the average time to calculate an angular distribution for one set of parameters is about 12 minutes, it was necessary to restrict the number of angular distributions to be analyzed. Three angular distributions were chosen to represent the main characteristics of the elastic scattering of alpha particles from nuclei; the monotonic decrease with increasing angle found in the heavy-element distributions, the diffraction structure in the light-element distributions, and the variations associated with changing the kinetic energy of the alpha particle. Approximately 100 different sets of the four parameters were tested for each of the three angular distributions.

Only very broad restrictions can be placed on each parameter. However, it is found that the parameters are important only so far as they combine together to determine the surface of the potential, i.e., where the potential is  $\geq -10$  Mev. Table I lists the parameters for the best potentials obtained. Figure 1 shows a plot of the magnitude of the real part of the best nuclear poten-

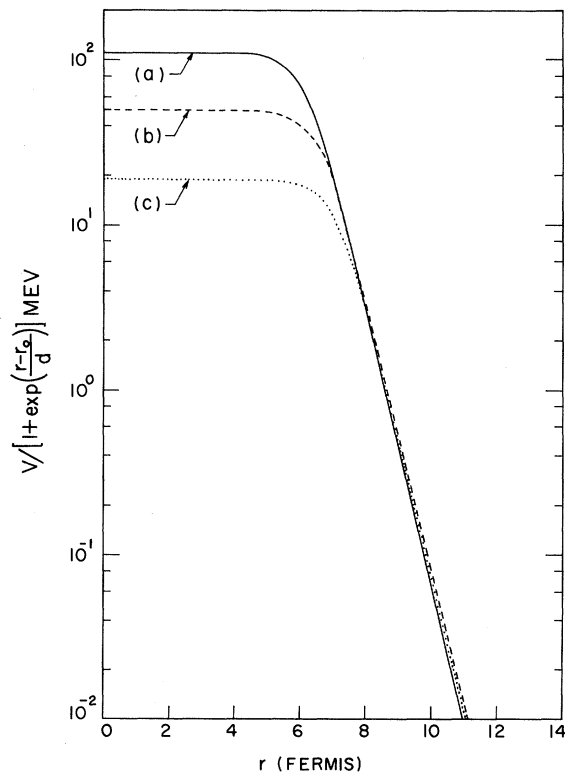


FIG. 1. Comparison of best real potentials for the elastic scattering of 40-Mev alpha particle from copper ( $V$  and  $W$  are in Mev;  $r_0$  and  $d$  in fermis). (a) ( $V, W, r_0, d$ ) =  $(-110, -20, 6.30, 0.5)$ ; (b)  $(-49.3, -11, 6.78, 0.5)$ ; (c)  $(-19, -13, 7.22, 0.5)$ .

TABLE I. The parameters in the nuclear potential,  $(V + iW)/\{1 + \exp[(r-r_0)/d]\}$ , obtained from this analysis.

Element	Kinetic energy of the alpha particle (Mev)	V (Mev)	W (Mev)	$r_0$ (fermis)	$d$ (fermis)
A	18	-87	-15	5.37	0.6
A	18	-40	- 8	6.05	0.5
Cu	40	-110	-20	6.30	0.5
Cu	40	-49.3	-11	6.78	0.5
Cu	40	-19	-13	7.22	0.5
Pb	48	-35	-15	8.71	0.6
Pb	48	-15	-10	9.30	0.6

tials as a function of radial distance for copper. These have one feature in common: the tails of the potentials are almost identical. The potential for  $V = -19$  Mev deviates from the other two at  $\sim 7$  fermis. This is in accord with the results of a least squares analysis which has been employed to judge the goodness of fit. The sum of residuals for the  $V = -19$  Mev potential is five times as great as the best of the other two. When other potentials which yield poorer fits are plotted, they deviate markedly in the region beyond 7 fermis from the three potentials in Fig. 1. These statements apply to the argon and lead analyses as well as the copper analysis.

When the nuclear surfaces obtained from the analysis of each element are compared, they are found to be identical within the limits of the accuracy of the analysis. In addition, the radial distance out to a point where the potential has a certain value in the range of 0 to -10 Mev follows an  $A^{1/3}$  law and consequently the surface of the real part of the nuclear potential can be represented as

$$-1100 \exp \left\{ - \left[ \frac{r - 1.17 A^{1/3}}{0.574} \right] \right\} \text{Mev}$$

for values  $\geq -10$  Mev, with  $r$  in fermis. The radial parameter,  $1.17A^{1/3}$  fermis, is larger than the radial parameter for the charge distribution,<sup>10</sup> and the surface thickness parameter, 0.574 fermis, is slightly larger than that of the charge distribution.

The corresponding imaginary potentials also agree in shape and quite closely in magnitude at the nuclear surface because the family of potentials chosen are such that real and imaginary parts have the same shape. The magnitude of the imaginary part is always large enough so that the central part of the nucleus is opaque. For instance, in the copper analysis the reaction

cross sections are 1711, 1708, and 1731 mb. The average value, 1717 mb, corresponds to a comparatively large area, 7.4 fermis in radius. Measurements of the total reaction cross sections of heavy elements would be useful in delineating the imaginary part of the potential more precisely.

It is concluded that alpha-particle elastic scattering experiments in the energy range 18 to 50 Mev are very sensitive to the surface of the nuclear potential, i.e., where the real nuclear potential is  $\geq -10$  Mev, but yield no information about the central part of the nuclear potential. The parameters which enter this analysis are important only insofar as they affect the surface of the nuclear potential and not at all as to how they affect the central real part of the nuclear potential. Further work is under way to study other families of potentials in which the real and imaginary part are not necessarily of the same form at the nuclear surface.

The author wishes to thank Dr. D. L. Hill, Dr. A. E. S. Green, Dr. K. W. Ford, and Dr. C. E. Porter for their continued support and interest in the program.

\*Work performed under the auspices of the U. S. Atomic Energy Commission and the Office of Naval Research.

<sup>1</sup> Seidlitz, Bleuler, and Tendam, Bull. Am. Phys. Soc. Ser. II, 1, 29 (1956).

<sup>2</sup> Igo, Wegner, and Eisberg, Phys. Rev. 101, 1508 (1956).

<sup>3</sup> R. Ellis and L. Schechter, Phys. Rev. 101, 636 (1956).

<sup>4</sup> R. D. Woods and D. S. Saxon, Phys. Rev. 95, 1617 (1954).

<sup>5</sup> D. L. Hill and K. W. Ford, Phys. Rev. 94, 1617 (1954).

<sup>6</sup> G. Igo and R. M. Thaler, Phys. Rev. 106, 126 (1957).

<sup>7</sup> Wall, Rees, and Ford, Phys. Rev. 97, 726 (1955).

<sup>8</sup> Wegner, Eisberg, and Igo, Phys. Rev. 99, 825 (1955).

<sup>9</sup> W. B. Cheston and A. E. Glassgold, Phys. Rev. 106, 1215 (1957).

<sup>10</sup> R. Hofstadter, Annual Review of Nuclear Science (Annual Reviews, Inc., Stanford, 1957), Vol 7, p 231.

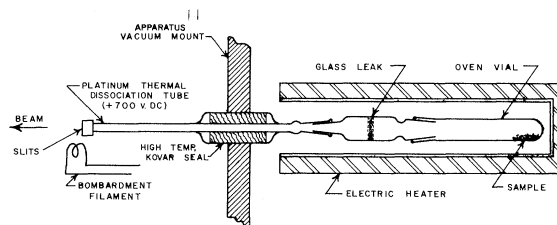
### NUCLEAR SPIN OF ASTATINE-211<sup>†</sup>

H. L. Garvin, T. M. Green, E. Lipworth  
Radiation Laboratory, University of California,  
Berkeley, California,  
and

W. A. Nierenberg

Miller Institute for Basic Research in Science,  
University of California, Berkeley, California  
(Received June 12, 1958)

In 1940 Corson, Mackenzie, and Segrè isolated a radioactive element whose chemical, physical and nuclear properties established it to be element 85, the last of the halogen group.<sup>1</sup> This element, which does not possess a stable isotope, was named astatine.<sup>2</sup> This note reports a measurement of the nuclear spin of one of the astatine isotopes, the 7.2-hr  $\text{At}^{211}$ , by the method of atomic beams. This measurement constitutes the first direct spin determination of an isotope, having no stable counterpart, whose half-life is measured in hours. It is of interest to note that each run was made with approximately  $10^{13}$  atoms of  $\text{At}^{211}$ . The  $\text{At}^{211}$  was produced by an  $(\alpha, 2n)$  reaction on a bismuth target in the Berkeley 60 in. cyclotron. A bombarding energy of 29 Mev was employed to preferentially produce  $\text{At}^{211}$  free of  $\text{At}^{210}$ . The astatine was separated from the target by evaporation; the target was heated to  $700^\circ\text{C}$  in air and the astatine collected upon a platinum foil. In order to produce an atomic beam, it was found necessary to mix the astatine with a natural carrier, and iodine was chosen because of the similarity of its chemical properties to those of astatine. The platinum foil was placed in an evacuated flask with approximately 200 mg of iodine and heated to drive off the astatine. An intimate mixing of the astatine and iodine was ensured by distilling the mixture several times from one end of the vial to the other. The atomic beam of astatine was produced by thermal dissociation of the At-I complex in a platinum tube heated by elec-



ASTATINE BEAM SOURCE

FIG. 1. Astatine beam source.

tron bombardment to approximately  $700^\circ\text{C}$  (Fig. 1). The astatine-iodine mixture was introduced into the platinum tube through a slow leak. The oven vial and associated glassware were maintained at a temperature of approximately  $100^\circ\text{C}$  to prevent absorption of the active material in the glass. With this arrangement, a 70% to 80% dissociated beam of astatine atoms was obtained. The beam was collected upon buttons coated with evaporated silver and detected by counting the decay  $\alpha$  particle in continuous-flow proportional counters.

The method used in this experiment is the atomic-beams "flop-in" technique due to Zacharias.<sup>3</sup> The apparatus used has been described elsewhere.<sup>4</sup>

In astatine the electronic configuration is  $6p^5$  and Hund's rule predicts that the ground electronic state is  $^2P_{3/2}$ . With this configuration and a nuclear spin  $I > 0$ , there are, with normal ordering of the hyperfine levels, two observable "flop-in" transitions. These are

$$(F = I + \frac{3}{2}, M_F = -I + \frac{1}{2}) \rightarrow (F = I + \frac{3}{2}, M_F = -I - \frac{1}{2}),$$

and

$$(F = I + \frac{1}{2}, M_F = -I + \frac{3}{2}) \rightarrow (F = I + \frac{1}{2}, M_F = -I + \frac{1}{2}),$$

where  $F$  is the total angular-momentum quantum number of the atom,  $I$  the nuclear spin quantum number, and  $M_F$  the projection of  $F$  along the direction of quantization. If  $g_F$  is the  $g$  factor of the particular  $F$  level in which a transition is observed at frequency  $\nu_x$  in a magnetic field  $H$ , we have

$$\nu_x \approx g_F \frac{\mu_0 H}{h}, \quad (1)$$

where  $\mu_0$  is the Bohr magneton and  $h$  is Planck's